 FDMP, vol.10, no.4, pp.443-464, 2014

Contribution to Improving the Performance of a Wind Turbine Using Natural Convection

M. Kriraa[1,2], M.EL Alami[1] and M. Abouricha[1]

Abstract: Natural Convection in a vertical channel with internal objects is encountered in several technological applications, among them particular interest of heat dissipation from electronic circuits, refrigerators, heat exchangers, nuclear reactors fuel elements, dry cooling towers, home ventilation, etc. This numerical study deals with the study of natural convection in a vertical convergent channel with a circular block. The considered parameters are $10^4 \leq Ra \leq 10^6$, Prandtl number $Pr = 0.71$, channel height $10 \leq A \leq 30$, inclination angle of the channel $\varphi = 0, 2.86^0, 5.74^0$. The size block conductivity and the block radius are assumed to be constant $\Lambda = 100$, $R = 0,1$ respectively. The Nusselt number and the mass flow rate are correlated with Rayleigh number. Further, the maximum kinetic energy (ΔV_{max}) is also evaluated.

Keywords: Convergent channel, Block, Natural convection, Numerical study.

Nomenclature

A	dimensionless channel height(H/b_{min})
b_{max}	inlet opening width
b_{min}	outlet opening width
H	channel height
q	heat flux imposed on the channel plates
M	mass flow rate
n	normal coordinate
Nu	mean Nusselt number (Case 1)
Pr	Prandtl number ($Pr = \upsilon/\alpha$)
r	block radius
R	dimensionless block radius $(r/b_{min}) = 0.1$

[1] Groupe De Thermique, LPMMAT, Département De Physique, Faculte Des Sciences Ain Chock, University Hassan II-Casablanca, BP 5366 Maarif, Casablanca, Morocco.
[2] Corresponding Author. E-mail: kriraa.m@gmail.com

Ra Rayleigh number ($Ra = g\beta q b_{min}^4/(\lambda_f \alpha \upsilon)$)
T temperature of fluid
T_c fluid temperature at the inlet, and on the block
θ dimensionless temperature of fluid=$(\lambda_r(T - T_c/q\ b_{min})$
u, v velocities in x and y directions
U, V dimensionless velocities in x and y directions =$(u, v)b_{min}/\alpha$
x, y cartesian coordinates
X, Y dimensionless Cartesian coordinates $= (x, y)/b_{min}$
α thermal diffusivity
β volumetric coefficient of thermal expansion
λ_f thermal conductivity of fluid
Λ thermal dimensionless conductivity of the block (λ/λ_f)
υ cinematic viscosity of fluid
ρ fluid density
φ channel plate inclination angle
Ψ dimensionless stream function

Subscripts

c cold
h hot
max maximum
min minimum
f fluid

1 Introduction

When it is shining, the wind strongly decreases, so the wind power gets very weak. We believe, there is a possibility to fix this well-known problem affecting wind turbines by modifying slightly the related convergent channel with a secondary turbine at the outlet. Plates of the channel are heated by solar radiation. Accordingly, in this study, we will show how it is possible to enhance the wind system efficiency by using natural convective flows.

In many applications it is advantageous to employ natural convection, since it is cheap, maintenance and noise free, and reliable, Peterson and Ortega (1990). The more frequently investigated configurations are the open cavities, Showole and Tarasuk (1993), Arid et al. (2012), horizontal channels, Lappa (2011), Compo et al. (1999), Rana et al. (2013) and vertical channels, Bilgen et al. (1995), Inclined

triangular, Mahmoudi et al (2013). Many kinds of thermal wall conditions are proposed to yield approximate conditions in the prediction of thermal performance of such configurations. Along the same lines, a numerical study of natural convection was conducted by Penot et al (2000). The authors considered a vertical channel which simulates a chimney placed in a closed and differentially heated cavity. The chimney walls capped isotherms. Natural convection in an asymmetrically heated channel with unheated extensions has been investigated experimentally by Manca et al. (2002). Average Nusselt number and maximum dimensionless temperature correlate to the Rayleigh number. A numerical investigation of free convection in a vertical isothermal channel was carried out by Desrayaud and Fichera (2002). Two rectangular blocks are symmetrically mounted on the channel surfaces. An experimental and numerical investigation of the effect of the position of wall mounted rectangular blocks on the heat transfer, taking into account the angular displacement of the block, was conducted by Bilen et al. (2001), Mahrouche et al. (2013). The experiments were conducted in a rectangular horizontal channel. Murakami and Mikic (2003), presented an optimisation study using a method of determining optimum values of the channel diameter, flow rate and number of channels for minimum pressure drop.

Among the most recent numerical studies of natural convection flows in a vertical channel there is one conducted by Wu-Shung et al. (2009). The particularity of this work is working with a large temperature difference between the heat source placed in the middle of one wall of the channel and the outside air temperature ($T_h =$ $606K$ and $594K$), while that of the surrounding medium was almost equal to $298K$. The Boussinesq approximation was no longer valid and it was not used in this case. In their results, the authors present a correlation of average Nusselt number based on the Rayleigh number. This correlation is similar to that encountered in the literature.

To our knowledge, there are no studies on the convergent channel containing an obstacle placed somewhere in the channel. However this configuration has in our opinion, many industrial applications. This makes our work original and important.

The paper is organized as follows. First, the studied configuration and the governing equations are introduced. Second, the numerical solution procedure for the full Navier-Stokes elliptic equations is also exposed. Later, in the last section of discussing the results, we explained validation of numerical results, the influence of Rayleigh number, channel height, converging angle, and a generalized correlation for kinetic energy, the average Nusselt number and mass flow rate.

2 Physical problem and governing equations

The physical domain under investigation is shown in Figure 1. It consists of two nonparallel plates with the block circular heat conducteur. Both plates are heated at uniform heat flux. The imbalance between the temperature of the ambient air and the temperature of the heated plates are drawn an air flow into the channel. The flow in the channel is assumed to be two-dimensional, laminar, incompressible. All thermophysical properties of the fluid are kept to be constant, except for the dependence of the density on the temperature (Boussinesq approximation), which gives rise to buoyancy forces. The convergent plates have a length H, the sections at the entrance b_{max} and exit b_{max}. Hence, the aspect ratio of the channel is h/bmin.

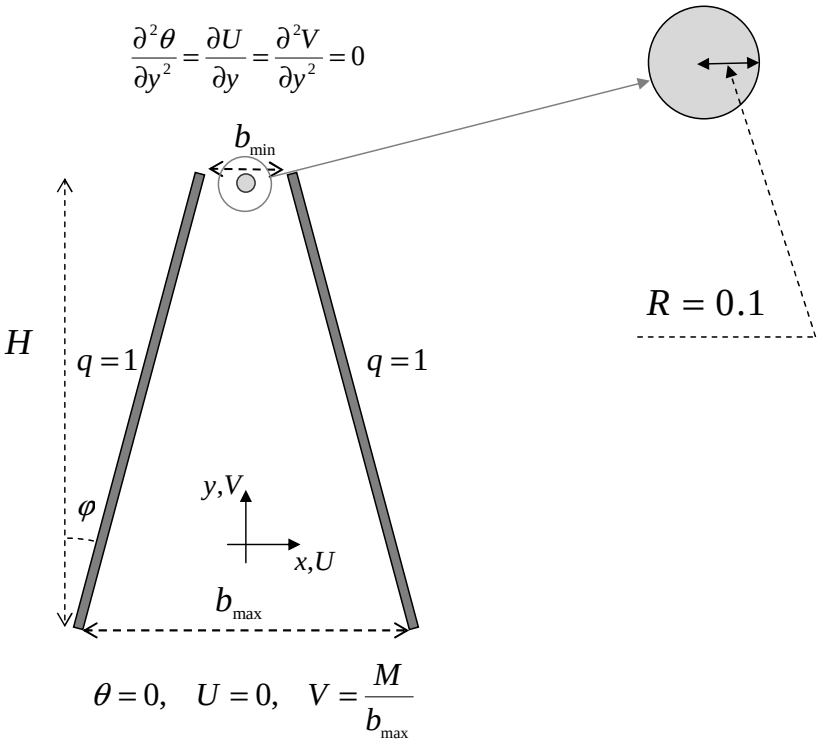

Figure 1: Sketch of the configuration and boundary conditions

The following variables and quantities are used for non-dimensional the governing equations and boundary conditions.

$$X = \frac{x}{b_{min}},\ Y = \frac{y}{b_{min}},\ \overrightarrow{V} = \frac{\overrightarrow{v}.b_{min}}{\alpha},\ t = \frac{t.\alpha}{b_{min}^2},$$

$$\theta = \frac{\lambda_r (T - T_r)}{q b_{min}}, \; P_M = \frac{(P + \rho \; g \; y) b_{min}^2}{\rho \alpha^2}$$

then the non-dimensional system of governing equations to be solved can be expressed as:

$$\frac{\partial U}{\partial X} + \frac{\partial V}{\partial Y} = 0 \tag{1}$$

$$\frac{\partial U}{\partial t} + U \frac{\partial U}{\partial X} + V \frac{\partial U}{\partial Y} = -\frac{\partial P}{\partial X} + Pr\left(\frac{\partial^2 U}{\partial X^2} + \frac{\partial^2 U}{\partial Y^2}\right) \tag{2}$$

$$\frac{\partial V}{\partial t} + U \frac{\partial V}{\partial X} + V \frac{\partial V}{\partial Y} = -\frac{\partial P}{\partial Y} + Pr\left(\frac{\partial^2 V}{\partial X^2} + \frac{\partial^2 V}{\partial Y^2}\right) + PrRa \; \theta \tag{3}$$

$$\frac{\partial \theta}{\partial t} + U \frac{\partial \theta}{\partial X} + V \frac{\partial \theta}{\partial Y} = \frac{\partial^2 \theta}{\partial X^2} + \frac{\partial^2 \theta}{\partial Y^2} \tag{4}$$

the two dimensionless numbers appearing in the governing equations are:

-the Rayleigh number

$$Ra = \frac{g \beta q b_{min}^4}{\lambda_r \nu \alpha}$$

-the Prandtl number

$$Pr = \frac{\nu}{\alpha}$$

The imposed boundary conditions, in terms of pressure and velocity, are similar to those of the natural convection flow in a vertical channel ($thermo - siphon$), Penot and Dalbert (1983) and Chappidi and Eno (1990):

- At the inlet opening:

$$P = -\frac{M^2}{2 b_{max}}, \; \theta = U = 0, \; V = \frac{M}{b_{max}}$$

- At the outlet opening:

θ *and* V are extrapolated by adopting similar processes as shown in references Tomimura and Fujii (1988),Najam et al (2004), El Alami et al(2008), and Tmartnhad et al (2008).

$$P = U = 0, \; \frac{\partial^2 \theta}{\partial Y^2} = \frac{\partial^2 V}{\partial Y^2} = 0$$

- On the channel plates: $q = 1$, $U = V = 0$

The mean Nusselt number over one active wall of the convergent channel:

$$Nu = \frac{1}{A}\int_{paroi}\frac{1}{\theta}dX \tag{5}$$

The mass flow rate is a fundamental unknown of this problem:

$$M = \int_{b_{min}} V dX|_{Y=A} \tag{6}$$

3 Numerical method

The governing equations of the problem were solved numerically using the control volume method of Patankar (1980). The QUICK scheme developed by Lionard (1979) was used for convective terms discretization Choukairy (2012), Maougal (2013) . The final discretized forms of the equations (1-4) were solved by using the SIMPLEC algorithm. Time steps considered ranging between 10^{-4} and 10^{-5}. The accuracy of the numerical model was verified by comparing our results with those obtained by De Val Devis (1983) and Le Queré (1985) for natural convection in differential heated cavity, Table 1, and then with the results obtained by Desrayaud and Fichera (2002) in a vertical channel with two ribs symmetrically placed on the channel walls, Table 2. We note good agreement in Ψ_{max} and M terms. When the steady state is reached, all the energy furnished by the hot walls to the fluid must leave the openings the channel through . This energy balance was verified by less than 5% in all cases considered here.

Note that the mass flow rate was rigorously equal to Ψ_{max}. The maximum deviation between M and Ψ_{max} which was equal to 0.7%, Table 2, confirm against the accuracy of our numerical code.

Table 1: Comparison of our results and those of De Val Davis (1983) and Le Queré and De Roquefort (1985).

Ra	De Val Davis (1983)	Le Queré and De Roquefort (1985)	Present study	Maximum deviation
10^4	$\Psi_{max} = 5.0980$	————	$\Psi_{max} = 5.035$	1.2%
10^5	$\Psi_{max} = 9.6670$	————	$\Psi_{max} = 9.725$	0.6%
10^6	$\Psi_{max} = 17.113$	$\Psi_{max} = 16.811$	$\Psi_{max} = 17.152$	2%
10^7	————	$\Psi_{max} = 30.170$	$\Psi_{max} = 30.077$	0.3%

On the experimental study of flows natural convection in a converging channel with block that was by Bianco et al (2007) Figure 2.

Table 2: comparison of our results and those of Desrayaud and Fichera (2002).

$Ra = 10^5$ $(A = 5)$	Desrayaud and Fichera (2002)	Present study	Maximum deviation
Ψ_{max}	151.51	152.85	0.9%
M	148.27	151.72	2.2%
Maximum deviation between M and Ψ_{max}	2.3%	0.7%	

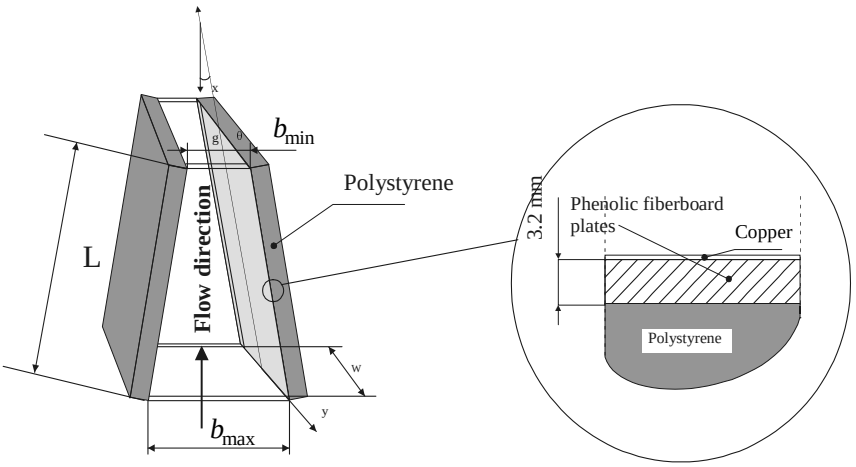

Figure 2: Experimental scheme designe by bianco and Manca (2007)

To validate any numerical model, the best scenario used is to compare the numerical results with those obtained experimentally in the same conditions applied. To achieve this goal, we chose the configuration studied Figure 2 since it is very close to our study. thus, the work we have done represents several numerical simulations respecting the design parameters used in the experimental part of Bianco et al. (2007)(inclination, aspect ratio and the Rayleigh range).

The average Nusselt number calculating along the heated wall of the channel was linear in logarithmic coordinates for the three angle values, and in the range considered Rayleigh number.

correlation giving the variation of the Nusselt according Rayleigh number is given and compared with that of Bianco (2007) (Figure 3).

In Figure 3, the dashed curve represents the correlation of Nusselt according to Rayleigh of the study Bianco (2007). The solid curve represents our Nusselt cor-

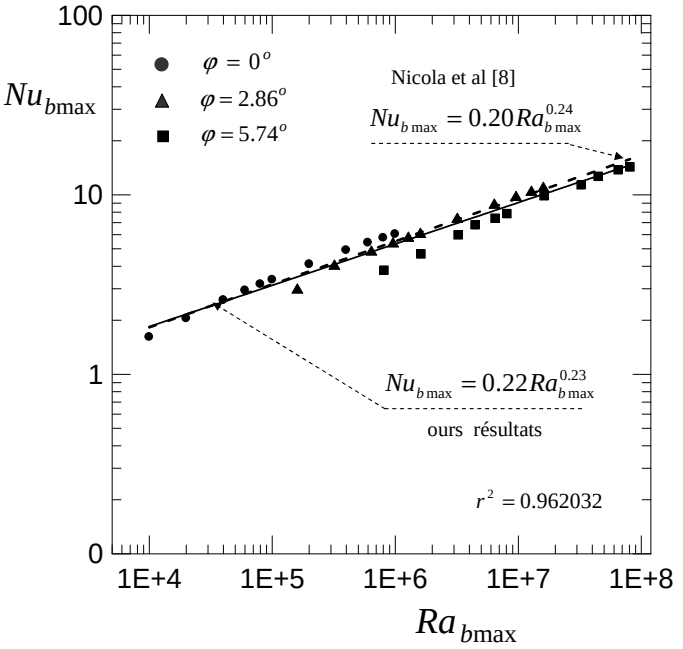

Figure 3: Comparison of numerical Nusselt number (our calculations) and experimental (Bianco et al (2007))

relation based on the Rayleigh number for three values of the angle $\varphi = 0°, \varphi = 2.86°, \varphi = 5.74°$. We note that there is a very good agreement between our results and those of Bianco (2007).

the maximum difference between the obtained correlation curves and points of numerical calculation is $\varphi = 5.74°$ and $3.10^5 \leq Ra \leq 5.10^6$ The same difference was founded by Nicola et al. (2007), which validates our fairly numeric code.

The following grid sizes: 80×200; 120×240 and 120×400 are used for the simulations respectively for $A = 10,\ 20$ and 30. A typical grid pattern for an aspect ratio of 10 is chown in figure 4.

4 Results and discussion

The heat transfer rate across the hot walls and the flow and temperature fields are examined for the Rayleigh number ($10^4 \leq Ra \leq 10^6$); channel height $A = 10,\ 20,\ 30$; channel plate inclination angle $0 \leq \varphi \leq 5.74^0$ and other parameters of the problem ($R = 0.1$, $Pr = 0.71$, $\Lambda = 100$).

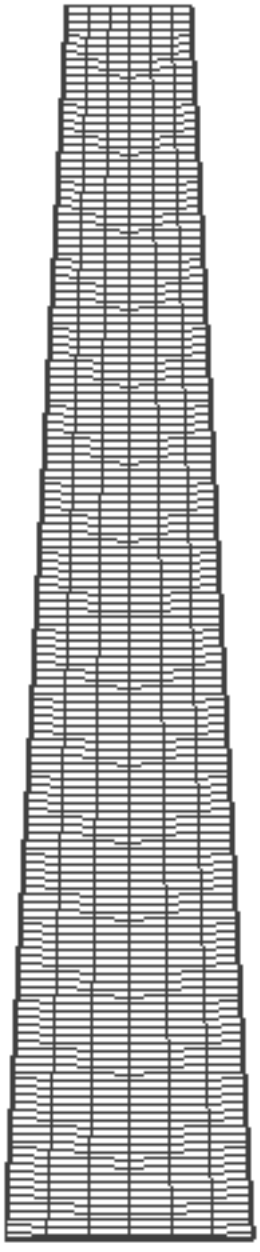

Figure 4: A typical grid pattern for an aspect ratio of 10

The particularity of this problem is the appearance of different solutions when varying Ra. The flow structure is composed of the open lines, which represent the aspired air by natural convection (thermal drawing), and closed cells which are due to the re-circulating movement inside the aspired of fresh air. The results of each of the runs $10^4, 10^5$ and 10^6 were checked in great detail to determine precisely the flow structure, thermal field and maximum air speed deviation introduced by the block existence.

4.1 Streamlines and isotherms

Useful information on velocity and temperature patterns in the channel for different control parameters, are given by the stream function and thermal fields presented in this section. Results are presented in two principal paragraphs: channel without block (only the case of $A = 10$ is presented) and channel with block at the outlet.

4.1.1 Channel without block: Case 1

The case of the channel without a block is not the objective of our work. So we present it in this section for $A = 10$, especially to give a comparison of the channel with block and to underline the effect the wall inclination angle. For $\varphi = 0$ and $Ra = 10^4$, fig.5-a, isotherms (on the left) which are not much distorted in the major part of the channel, show that the thermal drawing (buoyancy) is weak. Streamlines (on the right) are practically parallel to the channel planes. This solution is a $thermo-siphon$ type. The increase of Rayleigh number leads to an important jet of fresh air in the channel as reflected by the strong distortion of the isotherms and the high values of the stream function, fig.5-b, for $Ra = 10^5$:$|\Psi_{max}|_{Ra=10^5} = 38.78 > |\Psi_{max}|_{Ra=10^4} = 13.11$. This phenomenon is accentuated with Rayleigh number, as shown in fig. 5-c, for $Ra = 10^6$. In this case, $|\Psi_{max}|_{Ra=10^6} = 112$. Isotherms are too tight along the channel plates and present a good heat exchange through them. The channel is full by the open streamlines which are parallel to the hot walls, and the problem solution is always a $thermo-siphon$ kind.

For $\varphi = 2.86°$, figs.6-a, b, c, we present the flow structure and the thermal field. In the range of the low Ra values, we have raised the same solution that in the other case. The streamlines are not parallel, because of the channel convergence, but the solution is a $thermo-siphon$ kind and $|\Psi_{max}|_{\varphi=0} = |\Psi_{max}|_{\varphi=2.86^0} = 13.12$. fig.6-a, for $Ra = 10^4$. In figs.6-b and 6-c, we notice two mainly modifications in the flow structure. For $Ra = 10^5$, the streamlines show that, the boundary layer flow begins to be developed, especially in the lower part of the channel. Increasing Ra, advantageously, the streamlines and isotherms become tighter near the channel walls and show that the major part of fresh air jet passes close them,

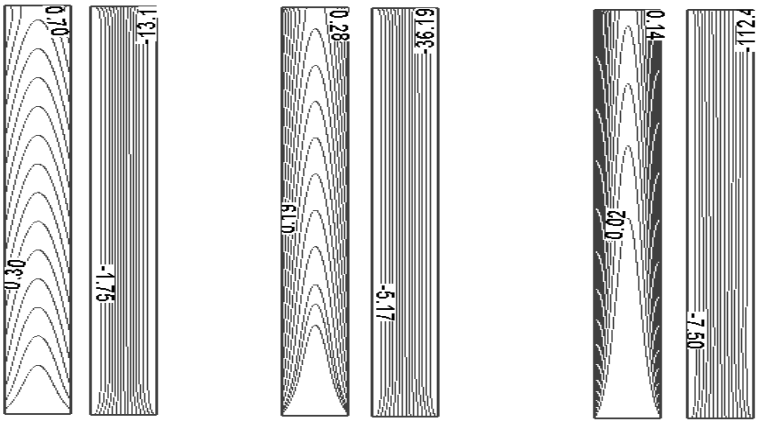

a)$Ra = 10^4$ *b*)$Ra = 10^5$ *c*)$Ra = 10^6$

Figure 5: flow structure and isotherms, $A = 10$, $\varphi = 0$, case 1.

fig.6-c, $Ra = 10^6$. Note that the thermal drawing, and so, fresh air aspiration is shortly affected by the wall inclination: compared to the case 1, the maximum of stream function is reduced for the same Rayleigh number value. For example, for $Ra = 10^5$,$|\Psi_{max}|_{\varphi=2.86^0} = 36.84 < |\Psi_{max}|_{\varphi=0} = 38.78$. In fig. 6-c, $Ra = 10^6$, we note that the isotherms are more tight near the hot walls than those of the case 1 (fig. 5-c). These isotherms show a slightly dissymmetric of the problem solution in the upper zone of the channel.

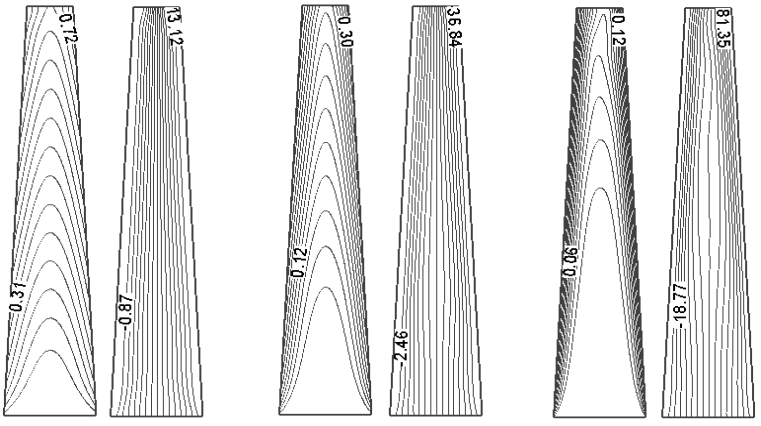

a)$Ra = 10^4$ *b*)$Ra = 10^5$ *c*)$Ra = 10^6$

Figure 6: flow structure and isotherms, $A = 10$, $\varphi = 2.86^0$, case 1.

In figs.7-a,b,c, have presented the problem solutions for $\varphi = 5.74^0$. For $Ra = 10^4$, there is a considerable change in the flow structure essentially in the lower zone of the channel: streamlines show the appearance of a re-circulating cell near the channel inlet. This flow re-circulating causes oscillations of the flow as can be seen on the corresponding isotherms in this zone, fig.7-a. For moderate and high *Ra* values, the re-circulating cell moves upward toward the middle of the channel, and it size increases as indicated in fig. 7-b and 7-c, for $Ra = 10^5$ and 10^6, respectively. The corresponding isotherms are too tight near the channel planes and present a minimum on the channel revolution axe. The separated boundary layer flow is installed and the problem solution, in these figures, is the *chimney effect* kind. One can notice, in fig. 7-c, that the streamlines present a slight asymmetry at the inlet zone. This phenomenon is not detected in previous cases. It is therefore, probably, caused by the increase of the inclination channel walls.

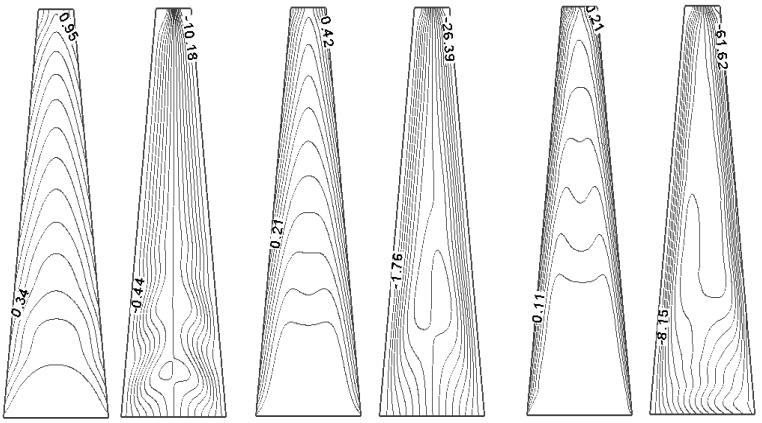

a)$Ra = 10^4$ *b*)$Ra = 10^5$ *c*)$Ra = 10^6$

Figure 7: flow structure and isotherms, $A = 10$, $\varphi = 5.74^0$, case 1.

4.1.2 Channel with block: Case 2

Note that in this section, we have not studied the case of $\varphi = 5.74^0$, because the width of the opening becomes smaller than the diameter of the block.

Generally, the block introduction has not changed too much the flow structure and the thermal field. It has, however, a limited effect in the vicinity of the block.

For $A = 10$ and $\varphi = 0$, the main point should be noted is the reduction of the buoyancy and the power of the jet caused by the obstacle existence, figs.8-a,b,c. To highlight this fact, compare these figures with those in paragraph 4.1.1, for

the same values of the control parameters (channel without block). For example for $Ra = 10^4$, we can notice the decrease of $|\Psi_{max}|$ value when introducing the block:$|\Psi_{max}|_{with\ bloc} = 9.71 < |\Psi_{max}|_{without\ bloc} = 13.11$. Note, also, that the isotherm value 0.37 (located lower than in the case without block), is placed down by 0.30 in the case 1. The same remark can be made if we compare figs. 5-b,c to those of the case 1.

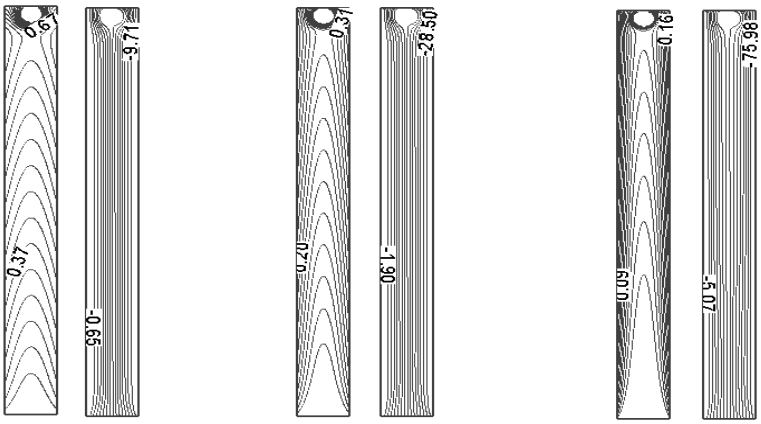

a)$Ra = 10^4$ *b*)$Ra = 10^5$ *c*)$Ra = 10^6$

Figure 8: flow structure and isotherms, $A = 10$, $\varphi = 0$, case 2.

In the convergent channel, $\varphi = 2.86^0$ figs.9-a,b,c, the major remark is the absence of the re-circulating cell for $Ra = 10^5$, fig. 9-b, and so there is no *chimney effect* for this *Ra* value, contrary to the case of the channel without block, fig.6-b. For $Ra = 10^6$ fig.9-c, the re-circulating cell appears again in the middle of the channel with a weak size, compared to the case 1. Note that the problem solution is symmetric.

To study the effect of the channel height, we varied A in the range $10 \leq A \leq 30$. We present for example the case of $A = 20$ in figs. 10-a,b,c, to discuss this parameter effect on the flow structure and thermal field. So, to highlight the effect of increasing A compare for example, figs.9. and 10. The first trivial remark it should be emphasized and is that the $|\Psi_{max}|$ values are much increased by the increase of A: $|\Psi_{max}|_{A=10} = 10.1 < |\Psi_{max}|_{A=20} = 16.60$, fig.10-a. We deduce that the increase of A significantly improves the buoyancy in the channel. Note, also, that the zone of convective cell development in the channel becomes very important in the case of $A = 20$. The cell appears earlier at $Ra = 10^5$, unlike the case of $A = 10$, and the development of the flow kind of separated boundary layers has already begun in the lower zone of the canal, fig.10-b. In the case of $Ra = 10^6$, fig.10-c, the cell occupies the major part of the channel and the *chimney effect* is important along the

hot walls, which improves the heat exchange through these planes.

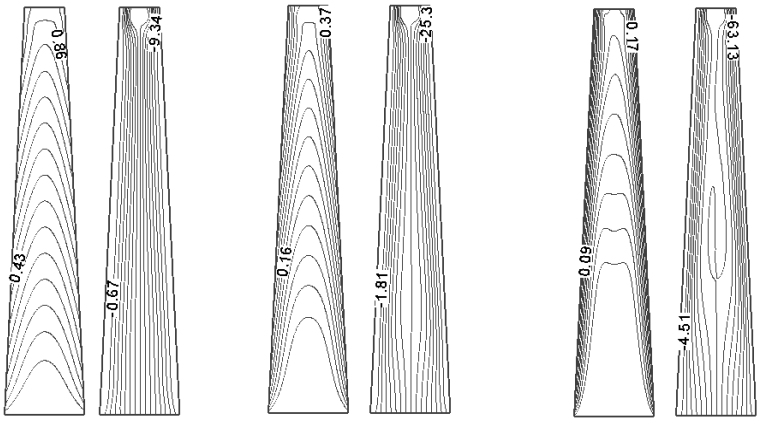

$a) Ra = 10^4$ $b) Ra = 10^5$ $c) Ra = 10^6$

Figure 9: flow structure and isotherms, $A = 10$, $\varphi = 2.86^0$, case 2.

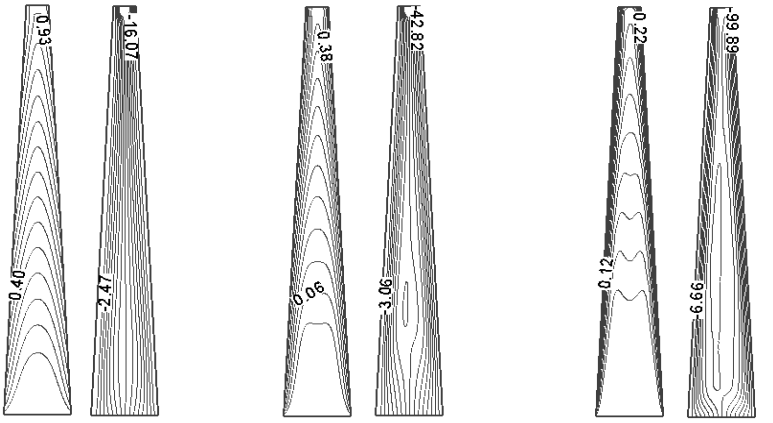

$a) Ra = 10^4$ $b) Ra = 10^5$ $c) Ra = 10^6$

Figure 10: flow structure and isotherms, $A = 20$, $\varphi = 2.86^0$, case 2.

4.2 Quantitative study of the problem

4.2.1 Kinetic energy of the flow

To get an idea about the energy of the convective flow can be transmitted to the turbine (simulated by the block), we evaluated the maximum difference between

velocities at the channel outlet with and without block

$$\Delta V_{max} = sup[(V_{without\ block} - V_{with\ block})_{Y=A}]$$

This gap variation with Rayleigh number, for various values of the channel height A, is shown in fig 11. First, we note that ΔV_{max} increases as a power law function (linear in logarithmic scale) of Ra for each value of A. Note then that ΔV_{max} increases with A dramatically. Each time we vary the height of the channel from A to $A+5$, ΔV_{max} increases by 50%, practically. For example, for $Ra = 10^5$, $\Delta V_{max} \approx 107$, that for $A = 15$ (for the same Ra value) is $\Delta V_{max} \approx 152$ and that for $A = 20$ is $\Delta V_{max} \approx 221$. So, more we increase the height of the channel, more we gain in kinetic energy may be converted into electrical one. We note with great interest, that ΔV_{max} variation in Rayleigh number, was correlated for each value of A and that the lines representing these correlations (logarithmic scale) are practically parallel with a slight variation of gaps between ΔV_{max} curves in the range of high Ra number. These correlations are obtained with errors do not exceed 6%.

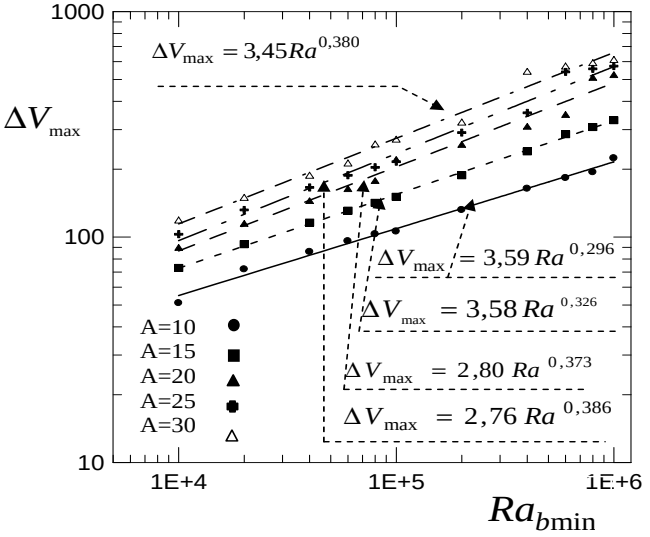

Figure 11: ΔV_{max} variation with Ra for different values of A

4.2.2 Heat transfer and masse flow rate

In this kind of geometries, and for the range of Rayleigh number chosen in this work, it has been found that it is more appropriate to use the minimum inter-plate spacing, according to the study conducted by Kim et al. (2000). As it has more

shown in the previous studies, a very good agreement with correlations for vertical parallel channels is reached if the results for the average Nusselt number versus *Ra* obtained are based on the opening at the top of the channel, b_{min}. This outlet opening means the physical exit section for the flow of fluid. Considering this remark, we conducted two ways to study heat transfer in terms of Nusselt number in the channel. It is initially to study the Nusselt number variation with *Ra*, for different values of the angle of the hot walls inclination. The results of this study are compared to the case of the channel without block. In the second procedure, we studied the variations of *Nu* as a function of *Ra* for different heights of the channel with block(case 2).

In the first hand, the mean Nusselt number variation with *Ra*, for different values of φ is presented in fig. 12. Generally, the Nusselt number increases, linearly in logarithm scales, with *Ra*. We have graphed *Nu* in the channel with and without the block versus *Ra*, in order to give a comparison of the two cases and to underline the effect of the block on heat transfer. Note that *Nu*(case1) is greater than *Nu*(case2). The gap between these curves decreases gradually with *Ra*. because the *chimney effect* is developed at high values of *Ra*, especially in the case 2: the major part of the flow pass close the walls and so the block effect on the heat exchange through the channel becomes limited as mentioned in the last paragraph. The maximum gap between the curves is observed at $Ra = 10^4$ and is equal to $\frac{(Nu(case1)-Nu(case2))_{max}}{Nu(case1)} \approx 22\%$. Note that in the case of the channel with the block, *Nu* variations with *Ra* for the two values of φ are practically identical and can be represented by the same curve. The *Nu* correlations proposed.

These correlations are obtained with a maximum deviation less than 6%.

In the other hand, we studied the heat exchange, in the Nusselt number term, with *Ra* for different values of the channel height, using the equation (5). The results of this study are shown in the fig 13. Contrary expected, the increase in the height of the channel leads to a considerable decrease of the Nusselt number, as shown in this figure, since the curve for $A = 10$ is above that of $A = 20$ which is over of that of $A = 30$. The study of the channel height effect on heat transfer in a convergent vertical channel has not studied yet, to our knowledge, and so we could not do a comparison. However, we can explain the decrease of *Nu* with more reduction of the width of the opening, which already contains the block. This reduction of b_{min}, caused by the inclination of the walls, when *A* increases, leading to a confinement of the flow, which penalizes the heat transfer in the channel. Note that in this case also, we propose correlations for *Nu* as a function of *Ra* for various values of *A*.

In table. 3 ,we present a comparison of our correlations and those of the literature in vertical smooth or ribbed channels.

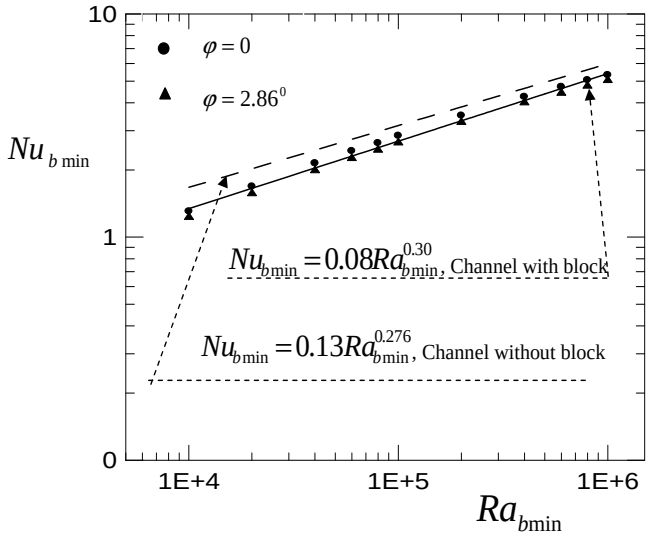

Figure 12: Nusselt variation with Ra for different angle inclination values, cases 1 and 2

Table 3: Comparison of our correlations with thoses of the literature

Kwak and Song(1998)	Acharya and Mehrotra (1993)	Tanda (1997)	Our correlations
$Nu = \alpha Ra^{\beta}$	$Nu_{bmin} = 0.41Gr^{0.25}$ (Smouth channel)	———	$Nu_{bmin} = 0.13Ra_{bmin}^{0.276}$
With $0.4 \leq \alpha \leq 0.46$ and $0.28 \leq \beta \leq 0.3$	$Nu = 0.36Gr^{0.25}$ (Ribbed channel)	$Nu = 0.41Ra^{0.25}$	$Nu_{bmin} = 0.08Ra_{bmin}^{0.300}$

4.2.3 Mass flow rate

The rate of induced mass flow is this other outcome of the problem. In fig. 14, we present M (eq.6) with Ra for different values of φ. As for the heat transfer, the mass flow variation is governed by a power law (linear log-log) function of Rayleigh number. In addition, it also decreases when more inclined walls of the channel because the outflow opening becomes smaller with increasing the inclination of the walls. A correlation equation based on the numerical results of this work are derived for different values of φ.

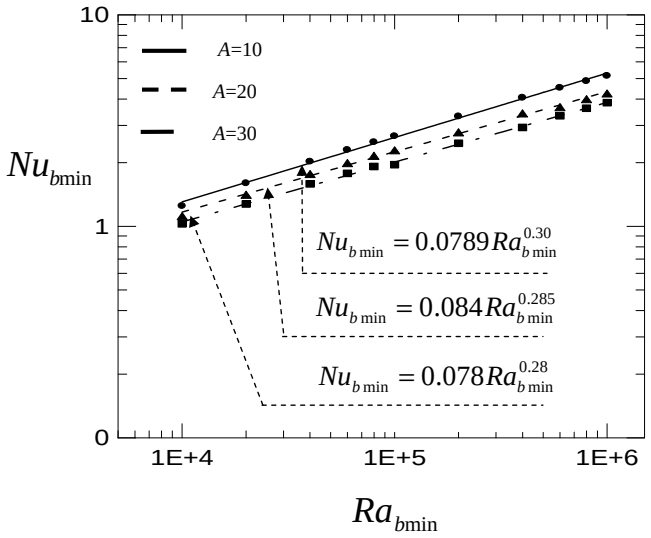

Figure 13: Nusselt variation with *Ra*, for different channel height values, case 2

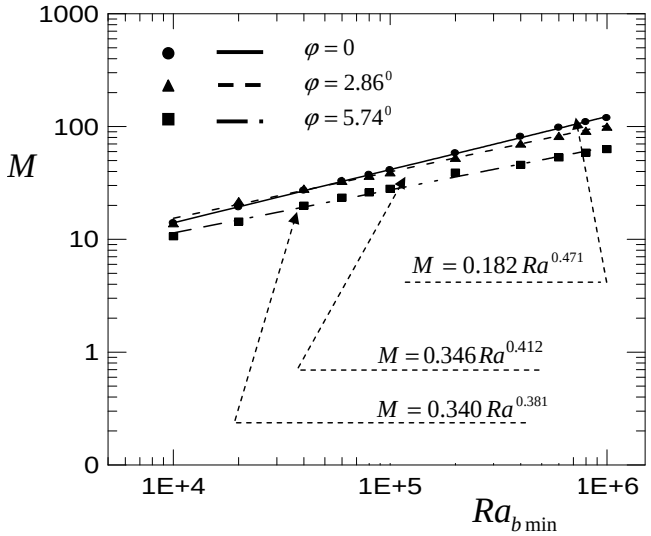

Figure 14: Mass flow rate variation with *Ra* for different values of φ

5 Conclusion

The main scope of this work was the identification of the conditions which may improve the performance of a wind turbine.

For this, we tried to assess the performances of a method to convert the kinetic energy of natural convection into electricity through a secondary turbine (simulated by a circular block) placed at the outlet of a convergent channel.

The numerical study, based on the finite volume method, enabled us to derive a set of conclusions which are summarized as follows:

- The inclination of the walls can lead to a reduction in power costs of the air stream (flow) and consequently a decrease in the Nusselt number and mass flow rate in the channel.
- One of the most important results of this study is that the kinetic energy of the flow in terms of ΔV_{max} increases considerably with the heating of the channel walls and its height. This allowed to properly size the system of wind power in order to improve its performance.
- Best correlations of results obtained for an average Nusselt number, ΔV_{max} the wall and the induced mass flow rate, were obtained by using the Rayleigh number based on the minimum inter-plate spacing.

References

Acharya, S.; Mehrotra, A. (1993): Natural Heat Transfer in Smooth and Ribbed Vertical Channels. *Int. J. Heat Mass Transfer, N°*1, vol. 36, pp. 236-241.

Arid, A.; Kousksou, T.; Jegadheeswaran, S.; Jamil, A.; Zeraouli, Y. (2012): Numerical Simulation of Ice Melting Near the Density Inversion Point under Periodic Thermal Boundary Conditions. *Fluid Dyn. Mater. Process,* vol. 8, no. 3, pp. 257-276.

Bianco, N.; Manca, O.; Nardini, S. (2007): Experimental investigation on natural convection in a convergent channel with uniformly heated plates. *Int J. of Heat and Mass Transfer,* vol. 50, pp. 2772-2786.

Bilen, K.; Yapici, S.; Celik, C. (2001): A Taguchi approach for investigation of heat transfer from a surface equipped with rectangular blocks. *Energy Convers Manage,* vol. 42, pp. 951-61.

Bilgen, E.; Wang, X.; Vasseur, P.; Meng, F.; Robillard, L. (1995): On the periodic condition to simulate mixed convection heat transfer in horizontal channels. *Numerical Heat Transfer, Part A,* vol. 27, pp. 461-472.

Chappidi, P. R.; Eno, B. E. (1990): A Comparative Study of the Effect of Inlet Conditions on a Free Convection Flow in a Vertical Channel. *Transactions of the ASME,* 1082/ 112.

Choukairy, K.; Bennacer, R. (2012): Numerical and Analytical Analysis of the Thermosolutal Convection in an Heterogeneous Porous Cavity. *Fluid Dyn. Mater. Process,* vol. 8, no. 2, pp. 155-172.

Compo, A.; Manca, O.; Morrone, B. (1999): Numerical analysis of partially heated vertical parallel plates in natural convection cooling. *Numerical Heat transfer, Part A,* vol. 36, pp. 129-151.

Desrayaud, G.; fichera, A. (2002): Laminar natural convection in a vertical isothermal channel with symmetric surface mounted rectangular ribs. *Int. J. Heat and Fluid Flow,* vol. 23, pp. 519-529.

De Vahl Davis, G. (1983): Natural Convection of air in a Square Cavity : A Bench Mark Numerical Solution. *Int. J. Numerical Methods in Fluids,* vol. 3, pp. 249-264.

El Alami, M.; Najam, M.; Semma, E.; Oubarra, A.; Penot, F. (2004): Chimney effect in a "T" form cavity with heated isothermal blocks: The blocks height effect. *Energy Conversion and Management,* vol. 45, pp. 3181-3191.

El Alami, M.; Semma, A.; Najam, M.; Boutarfa, M. (2008): Numerical Study of Convective Heat Transfer in a Horizontal Channel. *Journal of Fluid dynamics & material processing, N^{o}1,* vol. 5, pp. 1-9.

Kim, S. H.; Anand, N. K. (2000): Use of slots to enhance forced convective cooling between channels with surface-mounted heat sources. *Numerical Heat Transfer, Part A,* vol. 38, pp. 1-21.

Kwak, C. E.; Song. T. H. (1998): Experimental and Numerical Study on Natural Convection From Vertical Plates with Horizontal Rectangular grouves. *Int. J. Heat Mass Transfer, N^{o}16,* vol. 41, pp. 2517-2528.

Lappa, M. (2011): Some considerations about the symmetry and evolution of chaotic Rayleigh-Bénard convection: The flywheel mechanism and the "wind" of turbulence. *Comptes Rendus Mécanique,* vol. 339, pp. 563-572.

Le Quéré, P.; Alziary De Roquefort, T. (1985): Computation of Natural Convection in Two-Dimensional Cavities with Chebyshev Polynomials. *J. Computational Phtysics,* vol. 57, pp. 210-228.

Lionard, B. P. (1979): A Stable and Accurate Convective Modeling Procedure Based on Quadratic Upstream Interpolation. *Comput. Methods Appl. Mech. Eng,* vol. 19, pp. 59-98.

Mahmoudi, A.; Mejri, I.; Abbassi, M. A.; Omri, A. (2013): Numerical Study of Natural Convection in an Inclined Triangular Cavity for Different Thermal Boundary Conditions: Application of the Lattice Boltzmann Method. *Fluid Dyn. Mater. Process,* vol. 9, no. 4, pp. 353-388.

Mahrouche, O.; Najam, M.; El Alami, M.; Faraji, M. (2013): Mixed Convection Investigation in an Opened Partitioned Heated Cavity. *Fluid Dyn. Mater. Process,* vol. 9, no. 3, pp. 235-250.

Manca, O.; Musto, M.; Naso, V. (2002): Experimental analysis of asymmetrical isoflux channel-chimney systems. *International Journal of thermal Sciences,* vol. 42. pp. 837-846.

Maougal, A.; Bessaïh, R. (2013): Heat Transfer and Entropy Analysis for Mixed Convection in Discretely Heated Porous Square Cavity. *Fluid Dyn. Mater. Process,* vol. 9, no. 1, pp. 35-58.

Murakami, Y.; Mikic, B. B. (2003): Parametric Investigation of Viscous Dissipation Effects on Optimized Air Cooling Microchanneled Heat Sinks. *Heat Transfer Engineering,* vol. 24, pp. 53-62.

Najam, M.; El Alami, M.; Oubarra, A. (2004): Heat transfer in a "T" form cavity with heated rectangular blocks submitted to a vertical jet: the block gap effect on multiple solutions. *Energy Conversion and Management,* vol. 45, pp. 113-125.

Patankar, S. V. (1980): Numerical Heat Transfer and Fluid Flow. Hemisphere Publishing Corporation Washington D.C.

Penot, F.; Le Quere, P.; Cvejic, A. (2000): Convection naturelle dans le thermosiphon vertical confiné dans une cavité fermée. Journé e SFT convection en cavité de forme complexe.

Penot, F.; Dalbert, A. M. (1983): Convection naturelle mixte et forcée dans un thermosiphon vertical chauffé a lux constant. *Int. J. Heat and Mass Transfer, N^{o}11,* vol. 26, pp. 1639-1647.

Peterson, G. P.; Ortega, A. (1990): Thermal control of electronic equipment and device, in T. F. Irvine, J. P. Hartnett, Advances in Heat Transfer, vol. 2, Academic Press, NEW York.

Rana, G. C.; Thakur, R. C. (2013): Effect of Suspended Particles on the Onset of Thermal Convection in Compressible Viscoelastic Fluid in a Darcy-Brinkman Porous Medium. *Fluid Dyn. Mater. Process,* vol. 9, no. 3, pp. 251-266.

Showole, R. A.; Tarasuk, J. D. (1993): Experimental and numerical studies of natural convection with flow separation in upward-facing inclined open cavities. *Transaction of the ASME,* vol. 115, pp. 592-605.

Tanda, G. (1997): Natural convection Heat Transfer in vertical channels with and without transverse square ribs. *Int. J. Heat Mass Transfer, N^{o}9,* vol. 40, pp. 2173-2185.

Tmartnhad, I.; EL Alami, M.; Najam, M.; Oubarra, A. (2008): Numerical investigation on mixed convection flow in a trapezoidal cavity heated from below.

Energy Conversion and Management, vol. 49, pp. 3205-3210.

Tomimura, T.; Fujii, M. (1988): Laminar mixed heat transfer between parallel plates with localized heat sources, In proc. Int. Symp. On Cooling Technology for Electronic Equipment, Honululu, pp. 233-247.

Wu, C.; li, C. G.; Huang, C. P.; Huang, J. C. (2009): An investigation of a high temperature difference natural convection in a finite length channel without Bousinesq assumption. *Int. J. Heat and Mass Transfer,* vol. 52, pp. 2571-2580.